ELSEVIER

Chemical Engineering Journal 139 (2008) 264–271

Chemical Engineering Journal

www.elsevier.com/locate/cej

Removal of organic impurities with activated carbons for ultra-pure hydrogen peroxide preparation

Qian Lin [a,b], Yanbin Jiang [a], Jianming Geng [a], Yu Qian [a,*]

[a] *School of Chemical Engineering, South China University of Technology, Guangzhou 510640, China*
[b] *School of Chemical Engineering, Guizhou University, Guiyang 550003, China*

Received 16 March 2007; received in revised form 19 July 2007; accepted 27 July 2007

Abstract

The aim of this research was to select suitable activated carbon (AC) for effective removal of organic impurities from industrial aqueous hydrogen peroxide solution to produce ultra-pure hydrogen peroxide. The textural parameters and surface chemistry of four kinds of AC samples were measured and analyzed. Static and dynamic equilibrium adsorption experiments were carried out to compare the effect of AC on organic impurities adsorption and hydrogen peroxide decomposition. The effects of AC pore structure and surface chemistry on the adsorption of organic impurities were investigated. The fitting operation conditions, i.e., operating temperature and AC dosage, were also examined. The results showed that AC adsorption capacity on organic impurities from industrial aqueous hydrogen peroxide solution was mainly influenced by micropore structure of AC, as well as decomposition of hydrogen peroxide. The pore size of 1–3 nm is most effective for adsorption of organic impurities. It was found that the organic impurities in industrial hydrogen peroxide solution could be reduced effectively to meet the standard of ultra-pure hydrogen peroxide of SEMI-C8 level with the proposed AC and adsorption techniques.

Keywords: Ultra-pure hydrogen peroxide; Organic impurities; Activated carbon; Microporosity; Surface chemistry; Adsorption

1. Introduction

Ultra-pure hydrogen peroxide solution is one of the key chemical materials for wet chemical process in the microelectronic industry. It is mainly used for silicon wafers cleaning, etching, as well as photoresist stripping. Purity and cleanliness of the hydrogen peroxide, therefore, are critical to yield, performance and reliability of the integrate circuit (IC).

Currently, ultra-pure hydrogen peroxide solution is prepared by purifying industrial hydrogen peroxide solution, which is usually produced using the anthraquinone method. The industrial hydrogen peroxide solution contains certain amounts of organic, inorganic and metallic compounds. The majority of organic impurities contained in the crude aqueous hydrogen peroxide solution are introduced with working solvents and soluble degradation products, including C_9–C_{10} aromatics, trioctyl phosphate (TOP), anthraquinone and its derivatives, etc. [1,2]. The total organic carbon (TOC) of the crude solution is usually above 100 mg/l. These impurities would be decomposed into water vapor and other substances on the silicon wafer surface. It results in increasing partial oxidation rate of silicon wafers and increasing thickness of the oxidized layer, consequently results in uneven silicon wafer and degrade the IC plates [3]. Therefore, in the ultra-pure hydrogen peroxide the total organic carbon concentration has to be lower than 20 mg/l [4]. In the current industrial practice, distillation [5], adsorption and ion exchange resins [6–8], recrystallization [9], supercritical extraction [10] and membrane separation [11,12] are adapted to remove the organic impurities in preparing ultra-pure hydrogen peroxide solution.

The adsorption-based purification technique has attracted a great interest due to simplicity of equipment, mild process condition, as well as easy operation. Among adsorbent materials, activated carbons are unique and versatile adsorbents due to their huge surface area, unique microporosity, and varied adsorption effect. Amodeo and Naldini [6] developed a technique of purification organic impurities contained in hydrogen peroxide solution with activated carbon, which preliminarily partially deactivated the activated carbon by adsorbing there on an organic material. Kersey [13] disclosed a purification process

* Corresponding author. Tel.: +86 20 87113046.
E-mail address: ceyuqian@scut.edu.cn (Y. Qian).

1385-8947/$ – see front matter © 2007 Elsevier B.V. All rights reserved.
doi:10.1016/j.cej.2007.07.091

Nomenclature

C_0	organic impurities initial concentrations of hydrogen peroxide solution (mg/l)
C_e	organic impurities equilibrium concentrations of hydrogen peroxide solution (mg/l)
K_F, n	Freundlich constant
p	equilibrium pressure (Pa)
p_0	saturation pressure (Pa)
q_e	adsorbed amount of adsorbate per unit mass of adsorbent at equilibrium (mg/g)
V	volume of hydrogen peroxide solution (l)
W	mass of dry adsorbent used (g)

of hydrogen peroxide by using activated carbon, with chemically modification of activated carbon by using $(NH_4)_2CO_3$ or $(NH_4)_2$EDTA. Nevertheless, two main problems occurred in these purification processing. One is the purification efficiency of activated carbon. The other is the catalytic decomposition of hydrogen peroxide by activated carbons. And usually these two problems are conflicting.

Recently, it have been indicated that adsorption behavior of activated carbons in aqueous solution depends not only on the specific surface area or pore size distribution but also on the presence of surface functional groups [14]. And both the base material and activated conditions affect the pore structure and surface chemistry [14,15]. It is still required better understanding for the effects of the physical and chemical property of AC on adsorption of organic impurities.

The aim of this work is to select suitable activated carbon for effective removal of organic impurities from industrial aqueous hydrogen peroxide solution to produce ultra-pure hydrogen peroxide, with acceptable low catalytic decomposition of hydrogen peroxide. The effects of the pore structure and surface chemistry of AC on removal of organic impurities are investigated in this work. The decomposition of hydrogen peroxide during AC adsorption is discussed as well.

2. Experimental

2.1. Chemicals

Industrial aqueous hydrogen peroxide solution used in this study came from Guangzhou Jinzhujiang Chemical Co., China (H_2O_2 35.4%, TOC 140.287 mg/l, free acid 0.043%, residue after evaporation 0.020%, stability 99.3%). Ultra-pure water (resistance rate > 18.2 MΩ) was used. Other chemicals and reagents used were of analytical grade.

2.2. Preparation and characterization of activated carbon

Four kinds of activated carbons manufactured from relatively heterogeneous base materials of sawdust (sawdust AC), lignite (lignite AC), coconut shells (coconut AC), and wood (wood AC) were used in this study. The granular activated carbons were pulverized to micro-size powder, and then were screened to get AC powder samples within two sieves with opening of 75 and 45 μm. The AC samples were washed with ultra-pure water to remove soluble components, and then were dried at 378 K for 24 h using a vacuum drier before the experiments.

Nitrogen adsorption isotherms of AC samples were measured with an accelerated surface area and porosimetry system (ASAP 2010, Micromeritics Inc. Corp., USA) with nitrogen adsorption principle (at 77 K, and relative pressure p/p_0 from 10^{-6} to 0.995 range). The samples were heated to 473 K before the measurement, and then outgassed at the same temperature. The specific surface area (S_{BET}) of AC samples was calculated using standard Brunauer–Emmet–Teller (BET) equation [16]. The total pore volume, V_t, is calculated from the volume of nitrogen adsorbed at $p/p_o = 0.995$. The average diameter, D_p, is calculated as $4V_t/S_{BET}$ according to the cylinder pore model. The surface area and the volume of mesopores were calculated by Barrett–Joyner–Halenda (BJH) method [17]. The surface area and the volume of micropores were calculated by Horvath–Kawazoe (HK) method [18], while pore size distribution was calculated by density functional theory (DFT) [19].

Qualitative estimation of the surface functional groups of the AC samples was performed by a FTIR spectroscopy (Vector 33, Bruker Corporation, Germany) using potassium bromide (KBr) pellet method. The surface acidity of the AC samples was determined by Boehm method [20].

2.3. Adsorbing experiment of AC samples

Static and dynamic experiment AC adsorptions of organic impurities from hydrogen peroxide solution were conducted in batch systems. Varying dosages of AC samples and 100 ml of aqueous hydrogen peroxide solution were carefully fed to a series of 250 ml glass bottles. The bottles were sealed and then shaken at 288 K and a frequency of 140 rpm using a thermostat shaking bath. Adsorbing time is 2 h for static experiment, and varying from 20 min to 3 h for dynamic experiment. The adsorbed amount of adsorbate per unit mass of adsorbent at equilibrium, q_e (mg/g), was calculated as

$$q_e = \frac{(C_0 - C_e)V}{W} \quad (1)$$

where C_0 and C_e (mg/l) are the organic impurities concentrations of hydrogen peroxide solution at initial and equilibrium, respectively. V is the volume of hydrogen peroxide solution (l), while W is the mass of dry adsorbent used (g).

Experiment of influencing factors of AC adsorption was conducted in the same batch systems with 1 h of adsorbing time and 140 rpm of shaking frequency by changing dosage of AC, experimental temperature, initial TOC of hydrogen peroxide solution.

All experiments were repeated three times under the same conditions to confirm the repeatability. All samples were filtered to separate the filtrate and AC fines after adsorption. The residual concentration of organic impurities in filtrate was determined using TOC analyzer (OI Analytical 1020A,

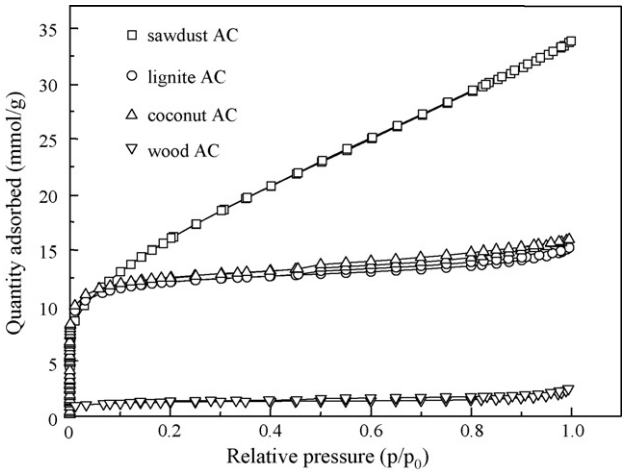

Fig. 1. Nitrogen adsorption isotherms of AC samples.

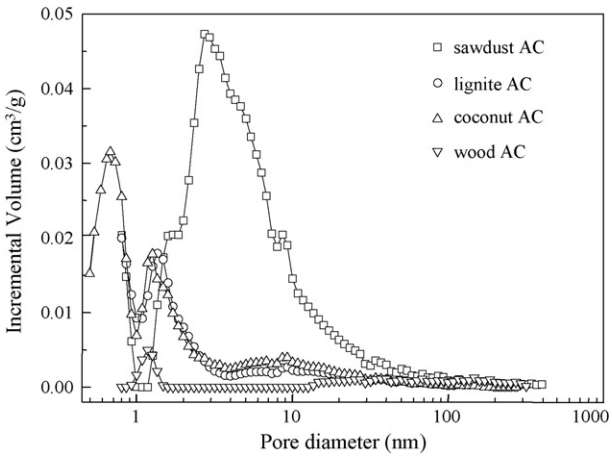

Fig. 2. DFT pore size distribution of AC samples.

USA). Hydrogen peroxide concentration analysis follows the specifications and guidelines for hydrogen peroxide (SEMI C30-0699).

3. Results and discussion

3.1. Pore structures of activated carbons

According to IUPAC classification, pores within porous materials are classified as micropore (width less than 2 nm), mesopore (width between 2 and 50 nm), and macropore (width greater than 50 nm). The nitrogen adsorption isotherms of four AC samples are shown in Fig. 1; it indicates the differences in porous structures. The nitrogen adsorption isotherm of sawdust AC sample shows that the adsorbed nitrogen volume increases with the rise in the relative pressure; it suggests that sawdust AC has micro-, meso-, and macropores. The nitrogen adsorption isotherm of lignite AC and coconut AC have similar shape, both have a steep region at low p/p_0, and the adsorbed amount of nitrogen increases slowly and approaches a limiting value as $p/p_0 \rightarrow 1$; these suggest the domination of micropores in pore structure for both lignite AC and coconut AC. The nitrogen adsorption isotherm of wood AC indicates that wood AC adsorbed only a little amount of nitrogen in entire pressure range; it suggests that the porous structure of wood AC is poor.

Fig. 2 shows DFT pore size distributions of four AC samples; it confirms the mentioned analysis of Fig. 1. According to Fig. 2, sawdust AC has a relatively extended pore size distribution, more than 90% of the pores are in range of 2–40 nm, and a small amount of micropores exist in range of 0.8–2 nm; it indicates that mesopores are dominant for sawdust AC. The pore size distribution of lignite AC concentrates in range of 1–3 nm, where a peak at 1.2 nm was observed, it indicates that micropores are dominant for lignite AC. Although the pore size distribution of coconut AC in range of 1–3 nm is similar to that of lignite AC, there is another peek at range of 0.5–1 nm; thus, the pore size distribution of coconut AC is broader than that of lignite AC. Fig. 2 also indicates that pores in wood AC are poorly developed.

The parameters of the porous structure of four AC samples are shown in Table 1, where S_{BET} is specific surface area; V_t is total pore volume; D_p is average pore diameter; S_{mi} and V_{mi} are micropore surface area and micropore volume, respectively, calculated by H–K method; S_{me} and V_{me} are mesopore surface area and mesopore volume, respectively, calculated by BJH method.

Table 1 shows that S_{BET}, V_t, S_{me} and V_{me} of sawdust AC are larger than that of other samples, but S_{mi} and V_{mi} of sawdust AC are smaller than that of lignite AC and coconut AC. These indicate that lignite AC and coconut AC have more developed micropore structures than that of sawdust AC. According to Fig. 2, coconut AC has more micropores in range of 0.5–1 nm, although lignite AC and coconut AC have similar S_{mi} and V_{mi}, it can be deduced that the micropore volume of range 1–3 nm for lignite AC is larger than that of coconut AC. As shown in Table 1, all parameters of wood AC are far smaller than other samples. Consequently, the descending order of micropore volume in range of 1–3 nm is lignite AC > coconut AC > sawdust AC > wood AC, while the descending order of micropore surfaces is coconut AC > lignite AC > sawdust AC > wood AC.

Table 1
Parameters of pore structure for AC samples

Sample	S_{BET} (m^2/g)	V_t (cm^3/g)	D_p (nm)	H–K method		BJH method	
				S_{mi} (m^2/g)	V_{mi} (cm^3/g)	S_{me} (m^2/g)	V_{me} (cm^3/g)
Sawdust AC	1336.8	1.16	3.47	1873.0	0.24	1183.9	1.15
Lignite AC	918.7	0.51	2.24	2303.3	0.28	153.9	0.18
Coconut AC	952.5	0.54	2.28	2395.0	0.29	168.3	0.20
Wood AC	96.4	0.07	3.04	217.5	0.03	24.8	0.05

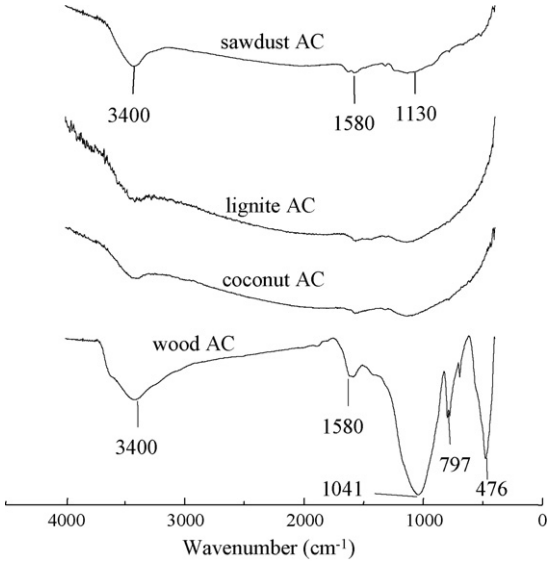

Fig. 3. FTIR spectrum of AC samples.

3.2. Surface chemistry of activated carbons

The FTIR spectra of AC samples are shown in Fig. 3. Because the concentration of the functional groups on the samples surface was low, the information obtained from FTIR spectrum was limited, but the absorption bands and peaks do provide evidence of the presence of some surface functional groups. The FTIR spectra of sawdust AC, lignite AC, and coconut AC are similar, and there are bands on their spectra at about 3400 cm^{-1} (assigned to the O–H stretching mode of hydroxyl functional groups), 1580 cm^{-1} (assigned to an aromatic ring stretching mode or a highly conjugated hydrogen bonded C=O [21], in analogous the structure of acetylacetone), and 1130 cm^{-1} (assigned to be due to carboxylic –OH group). It means that there could be the same functional groups on the surface of these AC samples. The FTIR spectra of wood AC differ from that of other three AC samples. Besides the bands at 3400 and 1580 cm^{-1}, two new bands appear at around 1041 cm^{-1} (assigned to C–OH stretching vibrations) and 797 cm^{-1} (assigned to C–H out-of-plane bending in benzene derivatives).

Table 2 shows the different surface functionalities per unit weight of AC samples, which were determined with Boehm's titration for evaluating surface chemistry effects on the adsorption of organic impurities from solution. It indicates that the amounts of oxygen complexes are tiny on the surface of four AC samples.

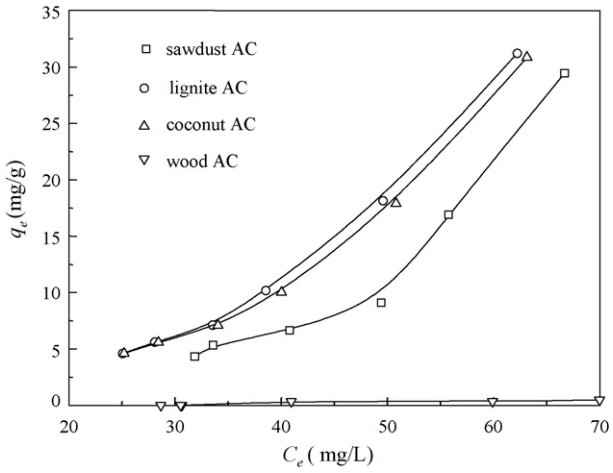

Fig. 4. Static adsorption isotherms of organic impurities on AC samples at 288 K.

3.3. Performance of different ACs

3.3.1. Static experiment

Results of static isotherm experiments for four AC samples are shown in Fig. 4, where C_e is the equilibrium concentration. It suggests that the adsorption capacity of AC samples is different. The adsorption isotherm of sawdust AC is much lower than that of lignite AC and coconut AC, and the isotherm of wood AC indicates that it has almost not adsorption capacity for organic impurities in hydrogen peroxide solution. The isotherm of lignite AC and coconut AC are similar, while the isotherm of lignite AC is above that of coconut AC. Therefore, the adsorption capacity is in the order of lignite AC > coconut AC > sawdust AC > wood AC. According to Table 1, the order of specific surface area and total pore volume is sawdust AC > coconut AC > lignite AC > wood AC. The adsorption capacity of sawdust AC is lower than that of lignite AC, and coconut AC, it suggests that adsorption capacities of AC samples are dominated by micropore structure but not specific surface area or total pore volume. Moreover, although S_{mi} and V_{mi} of lignite AC and coconut AC are almost the same, the isotherm data show that the adsorption capacity of coconut AC is lower than that of lignite AC, the reason is that coconut AC has a lot of ultra-micropores within 0.5–1 nm, but ultra-micropores do not play essential role in adsorption due to the exclusion of larger organic impurities from adsorbent pores [22].

Freundlich model were selected to fit the isotherm data, which is shown in Fig. 4. The well-known logarithmic form of Freundlich isotherm model is typically expressed as:

$$\log q_e = \log k_F + \left(\frac{1}{n}\right) \log c_e \quad (2)$$

Table 2
Results of Beohm titration for AC samples

Samples	Basic (mmol/g)	Acidic (mmol/g)	Carboxylic (mmol/g)	Phenolic (mmol/g)	Lactone (mmol/g)
Sawdust AC	0.0594	0.1135	0.0532	0.0246	0.0357
Lignite AC	0.0535	0.0361	0.0118	0.0138	0.0105
Coconut AC	0.1347	0.3624	0.1594	0.0968	0.1062
Wood AC	0.0758	0.0081	0.0015	0.0041	0.0025

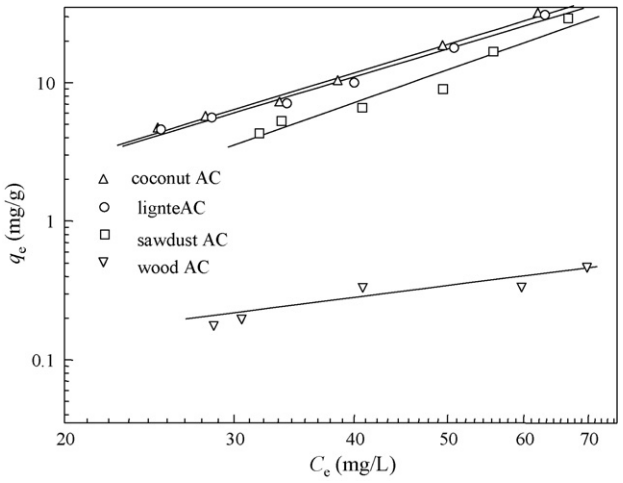

Fig. 5. Freundlich adsorption isotherm of TOC on AC samples at 288 K.

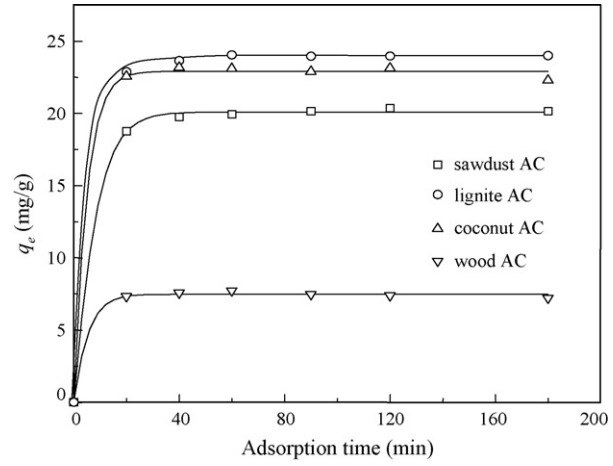

Fig. 6. Dynamic adsorption curves of organic impurities on AC samples at 288 K.

where K_F and n are Freundlich constants. Fig. 5 shows the fitting result. It can be found that Freundlich isotherm model satisfactorily fit the experimental data. Thus, Freundlich isotherm model is used for predicting this kind of adsorption systems. K_F and n are listed in Table 3.

3.3.2. Dynamic adsorption

Dynamic adsorption experiments were conducted to determine the equilibrium adsorption time for four ACS, where the adsorption time ranged from 20 min to 3 h at the same adsorption conditions. Fig. 6 shows the adsorption capacity versus the adsorption time for four AC samples at 288 K. According to Fig. 6, the equilibrium adsorption time for sawdust AC, lignite AC and coconut AC is about 60 min, and about 40 min for wood AC. Moreover, dynamic adsorption capacity of organic impurities on different AC is consistent with that of static isotherm experimental results, i.e., the adsorption capacity is in the order of lignite AC > coconut AC > sawdust AC > wood AC.

Table 3
Freundlich isotherm model constants for TOC onto AC samples

Sample	K_F ($\times 10^3$)	$1/n$
Sawdust AC	0.8437	2.452
Lignite AC	4.553	2.125
Coconut AC	5.121	2.080
Wood AC	7.593	0.966

Both static and dynamic isotherm data clearly illustrate that adsorption capacity of lignite AC is the best among the four AC samples. The results suggest that mesopores and macropores mainly act as feeder or transport pores during adsorption. As the order of adsorption capacity of AC samples is in agreement with the descending order of 1–3 nm micropore of AC samples, it suggests that micropores of 1–3 nm have remarkable effect on organic impurities adsorption.

According to Fig. 3 and Table 3, the FTIR spectra of sawdust AC, lignite AC, and coconut AC are similar, and the amounts of oxygen complexes are tiny on the surface of four AC samples. Consequently, it can be concluded from the above result that the effect of surface functionalities should be neglectable in this study. Thus, the dominative factors of adsorption behavior are the pore structure of AC sample in present work.

3.3.3. Decomposition of hydrogen peroxide

Hydrogen peroxide (H_2O_2) decomposition presents in all purification technologies because hydrogen peroxide is easy to decompose without stabilizing agent. How to control the decomposition of hydrogen peroxide in an acceptable range is an urgent technical problem for various purification technologies.

Fig. 7 presents the effect of different AC sample and its dosage on hydrogen peroxide decomposition during 1 h adsorption at 288 K. It indicates that the order of hydrogen peroxide decomposition for AC samples is coconut AC > lignite AC > sawdust AC > wood AC. This is consistent with the descending order of S_{mi} for AC samples, because the larger S_{mi} means more contacting chance between AC surface and hydrogen peroxide molecule. Therefore, it can be deduced that micropore surface area is the main feature leading to the decomposition of hydrogen peroxide.

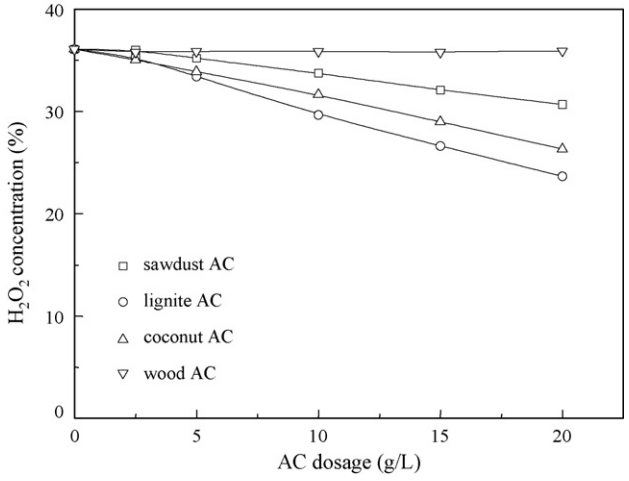

Fig. 7. H_2O_2 decomposition curve of AC samples at 288 K.

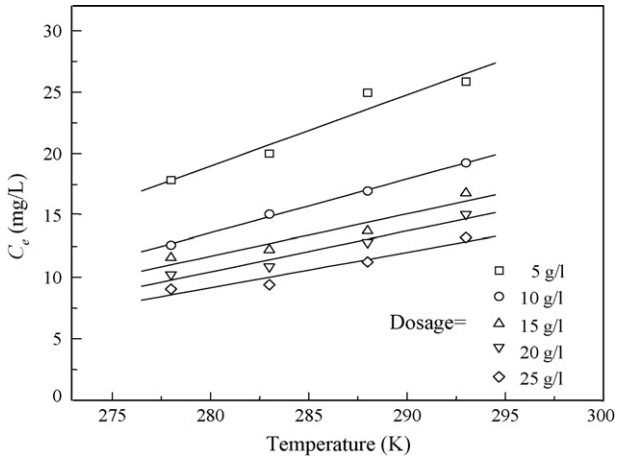

Fig. 8. Effect of temperature on adsorption equilibrium at various lignite AC dosages.

Synthetically considering adsorption capacity and decomposition of hydrogen peroxide, lignite AC was selected for further study.

3.4. Significant influencing factors of lignite AC adsorption

3.4.1. Effect of temperature and adsorbent dosage on lignite AC adsorption efficiency

To remove TOC from the H_2O_2 solution with AC, two selection criteria of AC should be taken into mind: larger adsorption capacity to reduce TOC content in the solution to below 20 mg/l and smaller H_2O_2 decomposition. Shown in Figs. 8 and 9 are TOC adsorption equilibrium concentration versus temperature, and H_2O_2 concentration versus temperature at various lignite AC dosages, respectively. From Figs. 8 and 9, it can be seen that, with the increase in temperature, the TOC adsorption equilibrium concentration increases, while H_2O_2 concentration decreased gradually at certain of lignite AC dosage. This indicates that temperature affects the adsorption equilibrium significantly; lower temperature facilitates the removal of organic impurities and lower H_2O_2 decomposition. Besides, as shown in Figs. 8 and 9,

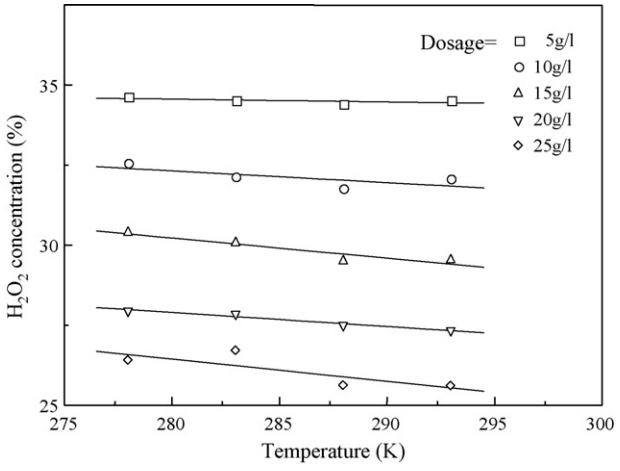

Fig. 9. Effect of temperature on H_2O_2 concentration at various lignite AC dosages.

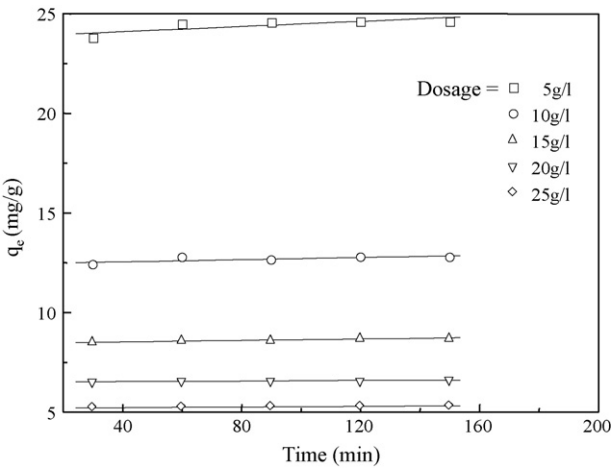

Fig. 10. Adsorption equilibrium curves at various lignite AC dosages at 278 K.

with the increase in lignite AC dosage, the TOC adsorption equilibrium concentration decreases, while H_2O_2 concentration decreases evidently. It shows that AC over-dosage may lead to H_2O_2 concentration loss, although it can reduce TOC equilibrium concentration. Therefore, the optimum working conditions should be chosen at lower adsorption temperature and lesser AC dosages. For this system, the adsorption temperature is determined at 278 K under the current experiment situation.

3.4.2. Effect of adsorption time and adsorbent dosage on lignite AC adsorption efficiency

Shown in Figs. 10 and 11 are the TOC adsorption equilibrium capacity curves and H_2O_2 concentration curves at various lignite AC dosages, respectively. From Figs. 10 and 11, we find that TOC adsorption equilibrium capacity increase slowly with the adsorption time. It reaches stable capacity in 60 min. On the other hand, H_2O_2 is reduced continuously over the time. It is realized from the data in Figs. 10 and 11 that AC over-dosages would be harmful in both aspects: not only affect the TOC adsorption equilibrium capacity, but also reduce H_2O_2.

Besides, it is observed in the experiments that the AC adsorption process is fluctuated and the data repeatability is

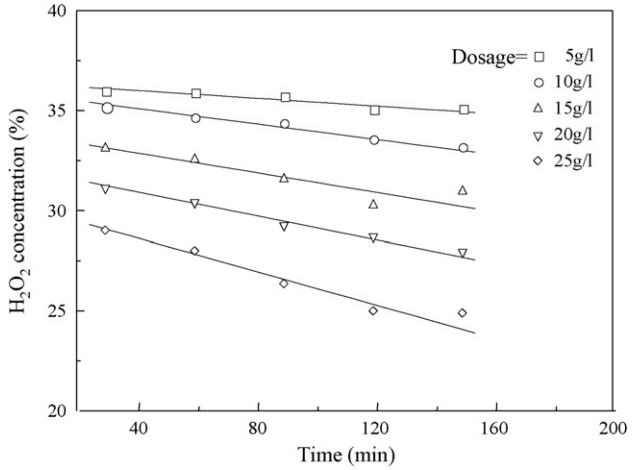

Fig. 11. H_2O_2 concentration curves at various lignite AC dosages at 278 K.

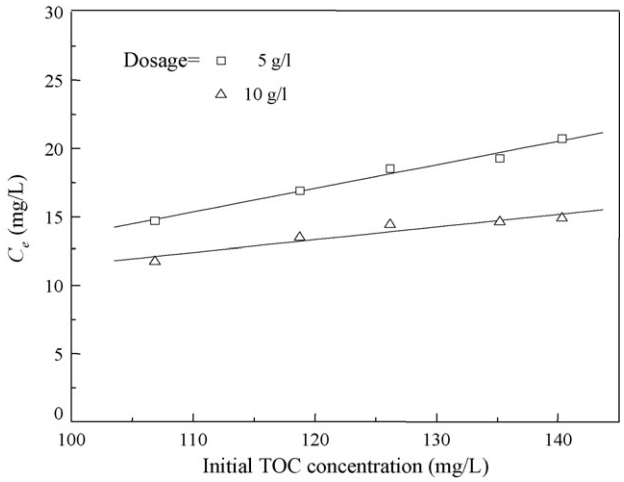

Fig. 12. Effect of C_0 and lignite AC dosage on C_e at 278 K.

unsatisfactory in the first 30 min. Therefore, 60 min adsorption equilibrium time is required for a stable adsorption process and satisfactory data repeatability for a meaningful analysis.

3.4.3. Effect of initial TOC concentration on lignite AC adsorption efficiency

Shown in Fig. 12 is the TOC adsorption equilibrium concentration (C_e) versus initial TOC concentration (C_0) at two lignite AC dosages. It indicates that C_e increased with the increase in C_0, i.e., the lower C_0, the better removal of organic impurities. When C_0 is less than 140 mg/l, C_e can be reduced to <20 mg/l with a lignite AC dosage of 5 g/l. Moreover, the effect of C_0 on C_e at lower amount of lignite AC dosage is more remarkable than that of higher dosage because the adsorption capability of AC decreases with the decrease in dosage.

3.4.4. Effect of lignite AC dosages on TOC and decomposition of H_2O_2 at 278 K

The effect of lignite AC dosage on TOC and decomposition of hydrogen peroxide at selected temperature of 278 K is studied; the result is shown in Fig. 13. It indicates that TOC in industrial grade hydrogen peroxide solution can be decreased to <20 mg/l

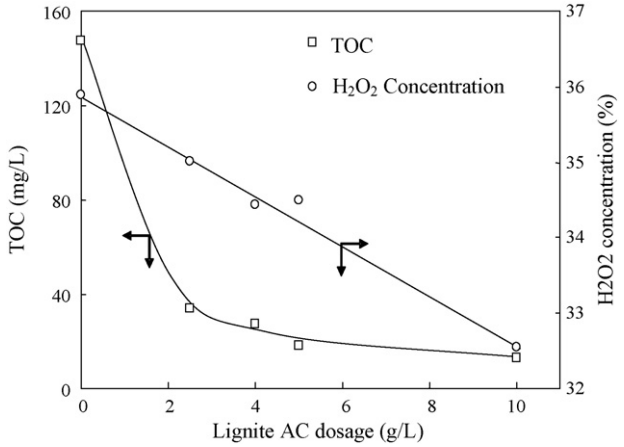

Fig. 13. Effect of lignite AC dosages on TOC and H_2O_2 concentration at 278 K.

only with a small lignite AC dosage of 5 g/l. Fig. 13 also indicates that the decomposition of hydrogen peroxide increases with the increase in lignite AC dosage. But when lignite AC dosage is within 5 g/l, concentration loss of hydrogen peroxide during adsorption process is less than 2%. In fact, no rapid catalytic decomposition phenomenon of hydrogen peroxide was found during adsorption using low lignite AC dosage.

According to the quality standards of electronic grade hydrogen peroxide solution [4], TOC upper limit of SEMI-C8 level is 20 mg/l. Therefore, TOC in industrial hydrogen peroxide solution can be conveniently and effectively reduced to meet the standard of high purity hydrogen peroxide of SEMI-C8 level with lignite AC. Moreover, the loss of H_2O_2 concentration is acceptable small during the purification process.

4. Conclusions

The present study shows that the removal of organic impurities of hydrogen peroxide depends mainly on micropores structure of activated carbon, while the effect of surface functionalities could be neglectable under the experimental conditions. And Freundlich isotherm model predicts this kind of adsorption systems satisfactorily.

The removal efficiency of organic impurities is greatly affected by micropores size distribution and micropores volume in range of 1–3 nm for activated carbon, while mesopores and macropores mainly act as feeder or transport pores during adsorption. The adsorption equilibrium between organic impurities and activated carbon is achieved within 60 min for all tested activated carbon samples.

Lignite AC is suitable adsorbent for removal of organic impurities from industrial hydrogen peroxide solution among the tested activated carbon samples. The adsorption efficiency of lignite AC increases with the decrease in adsorbing temperature, as well as the increase in lignite AC dosage. But higher dosage leads to higher decomposition of hydrogen peroxide. The results show that the suitable adsorbing temperature is 278 K, and the feasible dosage of lignite AC is 5 g/l. Also, the initial TOC concentration of industrial hydrogen peroxide solution has some effect on the adsorption process.

Using proposed activated carbon and adsorption conditions, TOC in industrial hydrogen peroxide solution can be conveniently and effectively reduced to meet the standard of high purity hydrogen peroxide of SEMI-C8 level, i.e., <20 mg/l, with a <2% H_2O_2 concentration loss.

Acknowledgements

Financial supports from the Natural Science Foundation of China (No. 20536020) and Guangzhou Municipal Bureau of Science and Technology (No. 2005Z3-D0171) are greatly appreciated.

References

[1] Q.D. Mu, The actuality, application, preparation and assistant technologies of ultra-clean and high pure chemical reagents, Chem. Reagents 24 (2002) 142–145.

[2] Q.L. Chen, High purity hydrogen peroxide, Inorg. Chem. Ind. 32 (2000) 22–24.
[3] R.M. Wen, Z.Z. Wang, Preparation and Detection Technology of Highly Pure Water, Science Press, Beijing, 1997.
[4] The North American Process Chemical Committee, Specifications and Guidelines for Hydrogen Peroxide (SEMI C30-0699).
[5] Y. Inaba, Y. Ueno, M. Watanabe, Y. Ishida, Process for preparing high purity hydrogen peroxide, US, 5670028[P] (1997).
[6] L. Amodeo, R. Naldini, Process for the purification of aqueous solution of hydrogen peroxide, US, 3399968[P] (1968).
[7] Y. Sugihara, Process for purification of hydrogen peroxide, US, 5614165[P] (1997).
[8] H.J. Honing, S.W. Geigel, Method for purifying hydrogen peroxide, US, 5232680[P] (1993).
[9] H. Ledon, C. Devos, Process for the preparation of an ultra pure hydrogen peroxide solutions by ion exchange in the presence of acetate ions, US, 6001324[P] (1999).
[10] I. Turunen, Method for purifying hydrogen peroxide, US, 5605670[P] (1997).
[11] J.M. Dhalluin, J.J. Wawrzyniak, H. Ledon, Process for the purification of hydrogen peroxide, US, 5851402[P] (1998).
[12] R.D. Crofts, J. Williams, Purification of hydrogen peroxide, US, 5215665[P] (1993).
[13] K. Kersey, Purification of hydrogen peroxide, US, 4985228 [P] (1991).
[14] S.J. Park, Y.S. Jang, Pore structure and surface properties of chemically modified activated carbons for adsorption mechanism and rate of Cr (VI), J. Colloid Interface Sci. 249 (2002) 458–463.
[15] S. Mukherjee, S. Kumarb, A.K. Misra, M. Fan, Removal of phenols from water environment by activated carbon, bagasse ash and wood charcoal, Chem. Eng. J. 126 (2007) 133–142.
[16] S. Brunauer, P.H. Emmet, F. Teller, Surface area measurements of activated carbons, silica gel and other adsorbents, Am. Chem. Soc. 60 (1938) 309–319.
[17] E. Barrett, L.G. Joyner, P.P. Halenda, The determination of pore volumes and area distributions in porous substances, J. Am. Chem. Soc. 73 (1951) 373–380.
[18] G. Horvath, K. Kawazoe, Method for the calculation of effective pore size distribution in molecular sieve carbon, Chem. Eng. Jpn. 16 (1983) 470–475.
[19] Z.Y. Ryu, J.T. Zheng, M.Z. Wang, Porous structure of PAN-based activated carbon fibers, Carbon 36 (1998) 42.
[20] H.P. Boehm, Some aspects of the surface chemistry of carbon blacks and other carbons, Carbon 32 (1994) 759.
[21] B.K. Pradhan, N.K. Sandlea, Effect of different oxidizing agent treatments on the surface properties of activated carbons, Carbon 37 (1999) 1323–1332.
[22] L. Li, P.A. Quinlivan, D.R.U. Knappe, Effects of activated carbon surface chemistry and pore structure on the adsorption of organic contaminants from aqueous solution, Carbon 40 (2002) 2085–2100.